



Electrochemical reduction of trichloroethylene using zero-valent iron bipolar packed-bed electrodes

Ja-Won Shin, Yu-Ri Park, Jeong-Joo Kim, Won-Ho Choi, Joo-Yang Park*

Department of Civil and Environmental Engineering, Hanyang University, 17 Haengdang-dong, Seongdong-gu, Seoul 133-791, Korea

Tel. +82 2 2220 0411; Fax: +82 2 2220 1945; email: jooyoungpark@hanyang.ac.kr

Received 23 March 2013; Accepted 5 May 2013

ABSTRACT

Bipolar electrode system has been known to be more efficient than monopolar electrode system in electrolytes of low electrical conductivity. In this study, the bipolar packed-bed electrodes system was investigated to degrade trichloroethylene (TCE) in groundwater which has a poor inherent conductivity of groundwater. Direct current was supplied to columns packed with sand and zero-valent iron (ZVI). The external current makes the ZVI granules in the column act as bipolar electrodes. As a result, TCE was reduced up to 72% with HRT of 62 min. On average, the TCE reduction in 0.13 mM lasted for the experiment period of 1100 h with the electric current of 20 mA. The dominant by-product was ethane, which is a final product of TCE reduction pathways. However, in the column without supplied current, TCE was barely reduced during the experiment. Low concentrations of dechlorinated hydrocarbons were detected compared with the column with current supply, with acetylene showing the highest concentration. No significant changes in chloride concentrations and pH were observed. The total dissolved iron concentration increased with decreasing TCE and vice versa for both columns.

Keywords: Trichloroethylene; Dechlorination; Bipolar electrode; Permeable reactive barriers

1. Introduction

Trichloroethylene (TCE) is commonly used as an industrial solvent and a metal degreasing reagent, but it is known to cause serious diseases such as cancer and congenital heart defects [1,2]. TCE evaporates quickly, when released into the environment because of its volatility. Also, once a large amount of TCE is

released from storage tanks, and pipes to the surfaces, it infiltrates the subsurface and migrates until it reaches an impermeable boundary, forming pools of contaminants because of its density (1.46 g/cm^3) and low K_{oc} (2.42). Furthermore, TCE persists for years in the environment, dissolving slowly from polluted groundwater [3]. Thus, there are many opportunities for accidental exposure to TCE by vapor from the water supply, and volatilization from groundwater through underground walls and floors and by

*Corresponding author.

contaminated groundwater [4]. There are different types of technologies for the removal of TCE such as air stripping for surface treatment and soil venting, bioremediation and permeable reactive barriers (PRBs) for subsurface treatment [3,5]. PRBs have been widely investigated and applied to subsurface remediation of groundwater containing TCE. The barriers may be filled with the mixture of reactive materials and nonreactive materials, such as sand. Since the ability of ZVI to degrade chlorinated compounds was verified by many studies [5–8], ZVI has been typically used as the reactive media of PRBs. Hydraulic conditions in the aquifer and the concentration of contaminant must be understood to determine the thickness of the barrier [9,10].

Recently, electrochemical degradation technology has received growing attention because the electrochemical reaction enhances the TCE degradation. Electrically induced reduction in saturated clay as well as in water contaminated with TCE was studied [11,12]. Results demonstrated that the TCE elimination rate constant increased with applied current. To improve the performances of PRBs, some researchers have coupled them with electrochemical degradation [13–15]. These studies have shown increased reduction rate and shortened half-life.

There are two ways to arrange electrodes for electrochemical processes, in monopolar or bipolar mode [16]. Most of the previous studies were carried out in monopolar mode (Fig. 1(a)). In monopolar mode, higher electric current flows [17] that requires additional high electrical conductivity. And also, it may intensify the aggregation problem of the ZVI filling part in a column with oxides, thereby obstructing the flow of water.

However, we have focused on bipolar mode (Fig. 1(b)). It consists of two feeders at both ends connected to a power source and other electrodes without any interconnections. In bipolar mode, on one

side of each bipolar electrode between two current feeders an anodic polarity is imposed, and on the other side, a cathodic polarity is imposed due to the potential difference between the electrolyte and the electrode. High voltage is applied to the two electrodes at both ends. In this case, electric current passing one electrode flows through the other electrodes; therefore, the total amount of electric current is low.

We considered bipolar packed-bed electrodes as an electrochemical PRB. The bipolar packed-bed electrodes consist of ZVI to react with TCE and sand to allow water to flow through the well. When electrical current is supplied, the ZVI granules in PRB become microconductors and act like bipolar electrodes [18]. Bipolar electrolysis is efficient with electrolytes of low electrical conductivity such as groundwater. Reactions also take place at main electrodes, as well as all over the reactor, where bipolar electrodes are placed.

The objective of this study is to determine the reduction capacity of bipolar packed-bed electrodes for TCE in groundwater by assessing, when ZVI acts as typical PRB media, and when ZVI acts as bipolar electrodes.

2. Materials and methods

2.1. Materials

ZVI and silica sand were prepared as packing materials to simulate PRBs. As a reactive material as well as a bipolar electrode, granular commercial ZVI of 40 mesh (Sang-Ah Blast, Korea) was chosen with no pretreatment before use. The ZVI granules contain 98.39–98.83% of Fe, 0.65–0.85% of Si, 0.14–0.18% of C, and minor impurities of Mn, P, and S. The sand (20–30 mesh, Joomoonjin Silica Sand Co., Ltd., Korea) was used to avoid reducing permeability due to the precipitation of (oxy)hydroxides of ZVI in the column and to keep ZVI isolated from each other. To remove impurities and dust, the sand was washed with deionized water prior to packing.

TCE (99.5%, Sigma–Aldrich) stock solution was prepared in methanol. Before the experiments, a glass bottle was filled with the TCE stock solution, 1 M of NaCl (99%, JUNSEI Chemical) to adjust the electrical conductivity of the solution in the range of 220–250 $\mu\text{S cm}^{-1}$ and deionized water to make the desired concentration (about 0.25 mM) without head space. And the solution in the glass bottle was stirred for two days to dissolve TCE completely. To minimize head space and evaporation, the TCE solution was transferred and stored in 10 L Tedlar[®] collapsible bags (SKC Inc.) during the experiments.

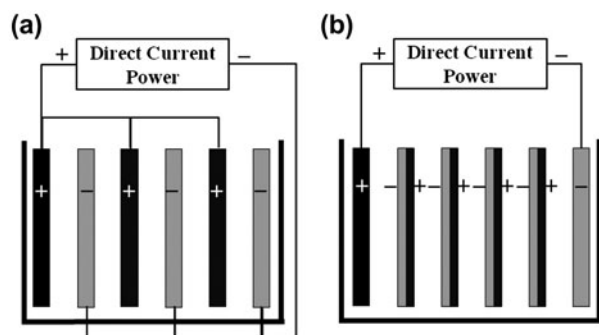


Fig. 1. Electrode arrangements: (a) monopolar and (b) bipolar in parallel connection.

2.2. Column experiments

Fig. 2 shows a schematic diagram of the experiments. Three cylindrical glass columns (L 300 mm, I.D. 46 mm) were prepared to avoid adsorption of TCE to the column walls. The first column was filled with sand only (column 1), the second was filled with sand and ZVI in a volumetric ratio of 2 to 1 (column 2), and the third was filled with the same amount of sand and ZVI as the second, but a constant voltage of 200 V was induced using a power supply (Sorensen) between the two main electrodes: the SUS 304 mesh cathode was positioned at the top of the column and the niobium mesh coated with platinum anode (Sun Wing Technology Co.) was positioned at the bottom (column 3). The electrodes were connected to the power supply with copper wires. Readings of the current were recorded every 5 min from the initiation of the experiment.

To minimize reactivity with TCE, a flexible tubing (Viton™) was used for a small part through the pump head, and Teflon tubing was used for all other connections. To stir the solution in the bag, four magnetic bars (D 2 × L 20 mm) were inserted through the inlet tap of the bag, and then, the TCE solution was transferred to the bag. The solution was kept in the bag and stirred on two magnetic stirrers during the experiments and delivered continuously to each column using a peristaltic pump (Cole-Parmer, Masterflex) at a flow rate of 2.3 ml/min. For sampling,

luer lock glass syringes were fitted to 3-way valves at each outlet of the columns at regular intervals. The syringe was filled with effluent as it flowed, and the rest of the effluent was collected in collapsible bags. Experiments were conducted at room temperature.

2.3. Analytical procedures

The samples from three columns were transferred in vials without headspace and centrifuged at 4,500 rpm for 5 min. To measure TCE concentration, 50 μl of the samples from the supernatant were extracted with 1 ml of hexanes (HPLC grade, J.T. Baker). Samples were analyzed with a gas chromatograph (GC-17A, Shimadzu) equipped with an electron capture detector according to the method 6232 of APHA [19]. A HP-5 capillary column (30 m × 0.25 mm i.d. × 0.25 μm film thickness, Agilent) was fitted to the equipment. The temperatures were 250°C for the injector and 280°C for the detector. The oven temperature was maintained at 60°C for 3 min and elevated to 150°C at a ramping rate of 15°C min⁻¹.

To analyze the hydrocarbons (acetylene, ethylene, and ethane), 2 ml of centrifuged samples were taken using a glass syringe and transferred to 5 ml vials. The vials were shaken in an orbital shaker for 5 min at 200 rpm and were left for 5 h to bring them to equilibrium between the liquid and gas phase. The samples were injected into a GC (YL 6100GC,

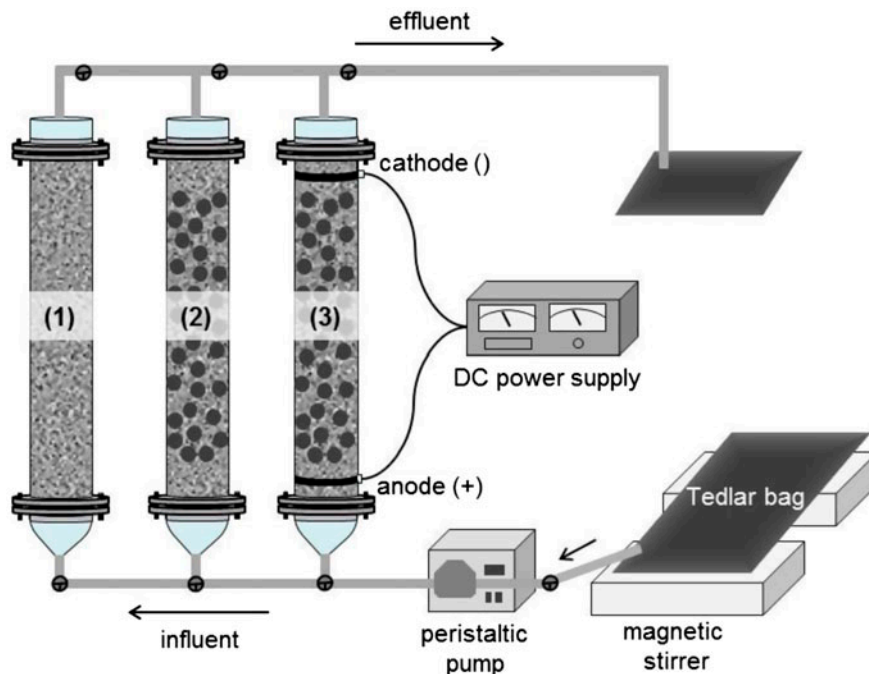


Fig. 2. Schematic diagram of experimental setup showing three columns. Column 1 is filled with only sand, column 2 is filled with sand and ZVI in a volumetric ratio of 2:1, and column 3 was filled with the same amount of sand and ZVI as column 2, but an electric current was supplied.

Younglin Instrument) equipped with a flame ionization detector, and a capillary column (HP-PLOT Q, 30 m × 0.32 mm i.d. × 0.20 μm film thickness, Agilent) for analysis. The modified analytical method was used based on the study of Berge [20]. The injector and detector were set at temperatures of 200 and 230 °C, respectively. The oven temperature was kept at 50 °C for 2 min and was increased 5 °C per minute up to 60 °C, and then the temperature was held for 2 min.

A calibration curve was generated and quality control samples were checked, when samples from experimental setup were analyzed. A HACH DR 2800 spectrophotometer was used to measure total iron, ferrous, and chloride. The pH and electrical conductivity were measured with a pH meter (Orion 720 A+, Thermo) and a conductivity meter (Orion three star, Thermo), respectively.

3. Results and discussion

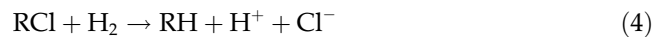
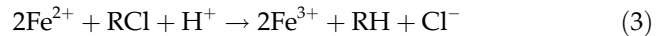
3.1. Effect of external current on TCE degradation

Fig. 3 shows TCE concentrations for the column experiments. Column 1 was run as a control to consider the effect of adsorption on sand and account for any losses. TCE concentrations of this column were 0.22–0.26 mM. TCE concentration for effluent of column 2 maintained 0.21–0.24 mM. Only 0.01–0.02 mM was reduced by ZVI compared with the TCE concentration of column 1. Because the ZVI was used without any treatment of the surface, the adsorption of TCE to the surface of ZVI was interrupted. Commercial iron is covered with Fe₂O₃ that is a passive layer

formed during iron production process at high temperature. The passive layer interrupts the reduction mechanisms of the contaminants involved in electron transfer and catalytic hydrogenation [6]. Some researchers have investigated the effect of pretreatment of the ZVI surface. They found that acid-washed ZVI showed faster reduction rates compared with unwashed or untreated ones [21,22].

TCE concentration was decreased from 0.25 to 0.1 mM at the beginning of the experiment, and this reduction lasted for 200 h in the column 3. This was significantly different from the results of column 2. ZVI was oxidized to Fe²⁺ and/or Fe³⁺, and the electrons that were produced degraded the TCE. In this study, granular ZVI was used instead of plate type for the bipolar electrode between the main electrodes, because it has a larger effective surface. Since ZVI granules in the column are isolated from each other, each granule acts as a bipolar electrode, which means it is possible that both oxidation and reduction can simultaneously occur on the same granule. Also, the ohmic drop is low since the cathode and anode are close to each other [23], and the granular bipolar electrodes are in vicinity of each other, indicating that the TCE migration distance is short. External current may promote the release of electrons from iron corrosion and hydrogen from water electrolysis [15]. This effect could initially improve the efficiency of TCE reduction, since ZVI, ferrous iron, and hydrogen contribute to dechlorination of TCE [24]. Electrolysis is the passage of a direct current through electrodes driving chemical reactions. The expected reactions in column 3 were as follows [17]:

Cathode



Anode

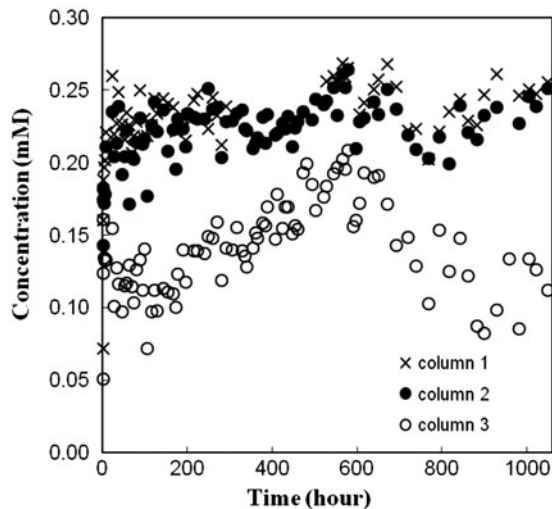
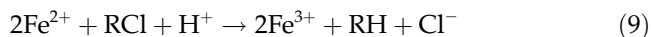


Fig. 3. TCE concentrations in effluents from the columns (column 1 (x), column 2 (•), column 3 (o)) as a function of time.



After 200 h, TCE concentration gradually increased to 0.19 mM until the experiment time of 700 h. The corrosion of ZVI resulted in lower degradation rates [25]. TCE degradation is a surface reaction, but over time, the blackish precipitation was observed through the column 3, and it covered the packing materials. It seemed that the precipitation was iron (hydr)oxide [15]. This caused not only a decrease in the reactive surface of ZVI but also prevented it from playing a role as a bipolar electrode. However, TCE concentrations again decreased. Even though the ZVI could not act as electrodes, iron oxides such as magnetite, [6] and green rust [13] covering the ZVI may allow electron transfer to occur. These oxides may cause TCE reduction in latter stages. The TCE reduction in column 3 tended to be activated with increases in current and vice versa (Figs. 3 and 4). Support for this finding can be found in previous studies that investigated increases in TCE elimination rate with induced current [11].

3.2. By-products of TCE degradation

The concentrations of dechlorinated hydrocarbons were measured during the experiment and plotted versus time (Fig. 5). Two columns showed different tendencies. Acetylene showed the highest concentration followed by ethylene and ethane (Fig. 5(a)) in column 2. Fig. 6 presents the pathways suggested for TCE

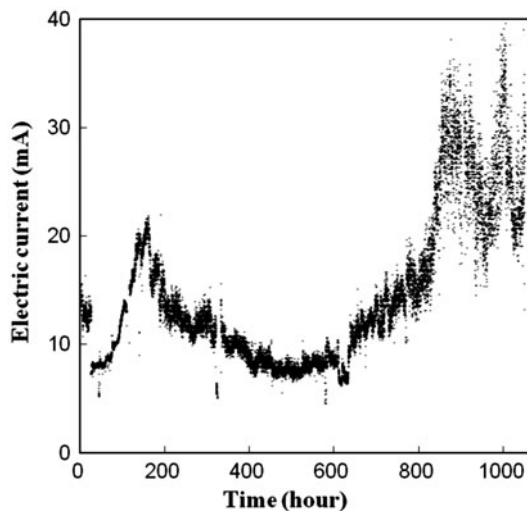


Fig. 4. Electric current in bipolar column at constant voltage of 200 V.

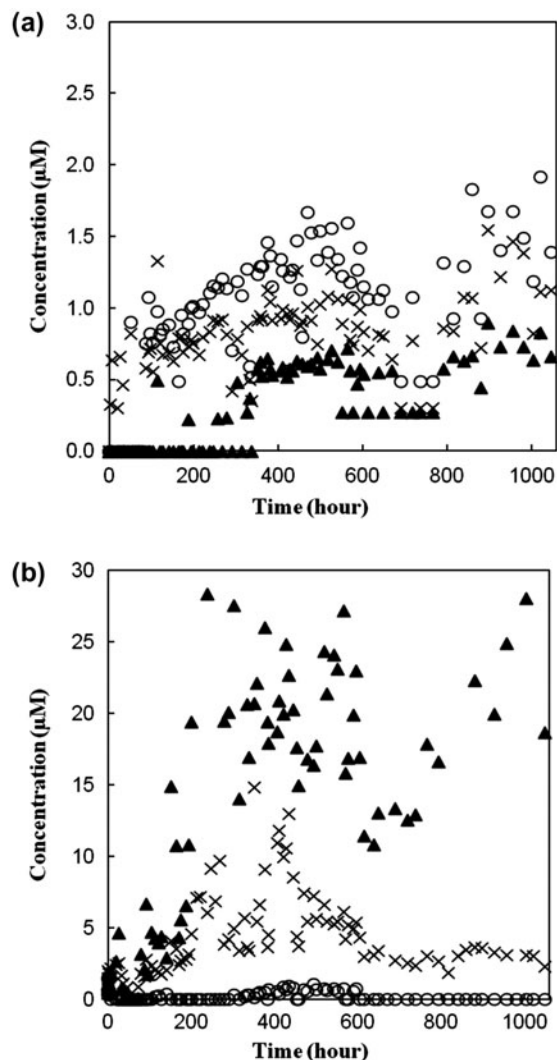


Fig. 5. Concentrations of dechlorinated ethylenes (\circ acetylene, \times ethylene, \blacktriangle ethane) from (a) column 2 and (b) column 3.

degradation [26]. Similar to the results of previous reports [26–28], column 2 underwent reduction to acetylene and ethylene. This indicates that the pathway follows reductive β -elimination as does most TCE degradation by ZVI. Column 3 showed about five times higher concentrations of ethylene on average compared with those of column 2. Except for a few samples, acetylene was not detected (Fig. 5(b)). Ethane was dominant and the concentrations were high. Further reactions were observed in column 3, since the external supply of electrical current increases reduction rate by providing electrons and hydrogen that are involved with TCE reduction [13]. TCE was initially reduced; therefore, we expected that most of the reduced may converted to dechlorinated hydrocarbons. However, lower concentrations of intermediates

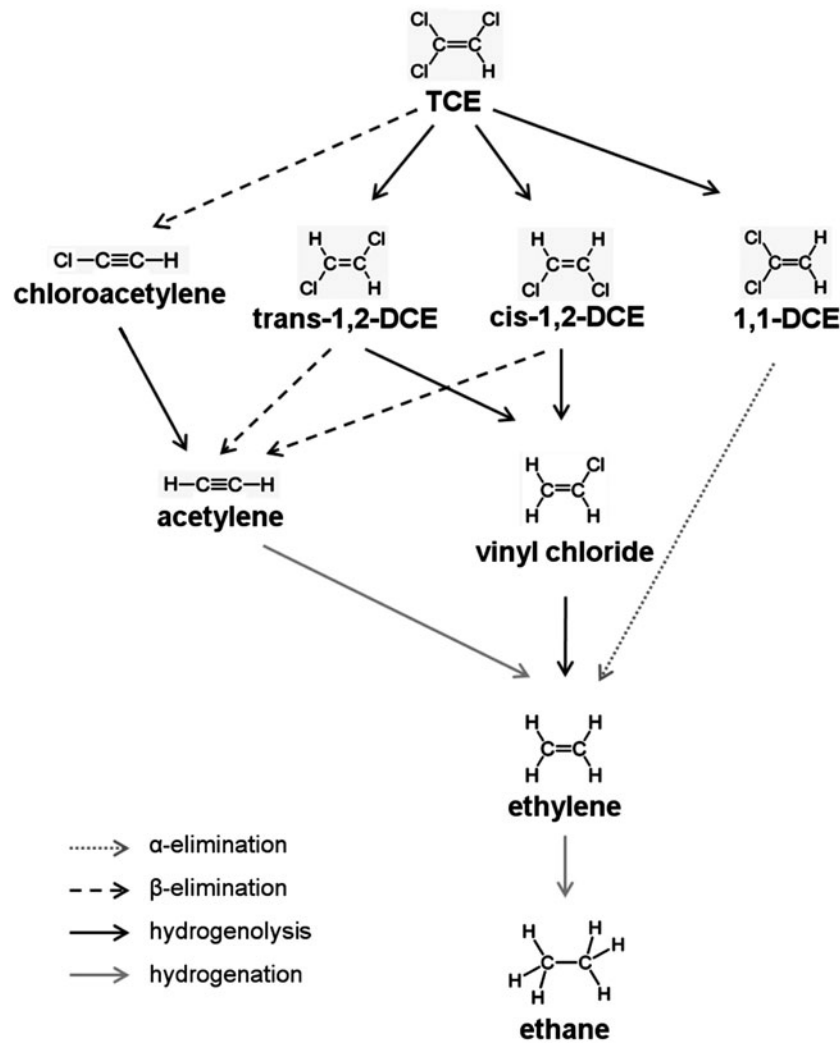


Fig. 6. Proposed pathways for reduction of TCE and other intermediates by ZVI [22].

were observed. Oxygen at the anode and hydrogen at the cathode were generated in the early stage of experiment, and the by-products such as ethylene and acetylene may be evaporated with the bubbles, since the by-products were unsaturated hydrocarbons.

3.3. Dissolved iron and chloride concentrations

Fig. 7 presents the concentrations of total dissolved iron, and soluble ferrous iron in the samples. In column 3, the concentrations of total dissolved iron were proportional to the concentrations of reduced TCE (Fig. 7(b)). Ferrous iron was rarely detected from column 2 and total dissolved iron showed low concentrations compared with that from column 3. This implied that the corrosion of ZVI involves, and Fe^{2+} could be an intermediate product of ZVI corrosion. Both involve in TCE reduction [24].

Fig. 8 shows chloride content in the effluents of all three columns. The chloride concentration of column 1 was approximately 1.2–1.8 mM due to the addition of NaCl for adjustment of electrical conductivity. Low concentrations of chloride were initially observed in column 2 and then, it showed slightly higher chloride concentration than those of the sand column after 200 h of experimental time. Though further experiment and analysis are required to clarify the exact mechanisms, it seemed that decrease in chloride concentration was caused by chloride sorption on the surface of ZVI.

The low concentration of chloride addition improved the dissolution rate of iron at pH 4 [29]. Iron dissolution is promoted by anions entering into the metal/water surface complex [30]. However, further increments of chloride ions increased the probability of immediate interaction with the metal and decrease

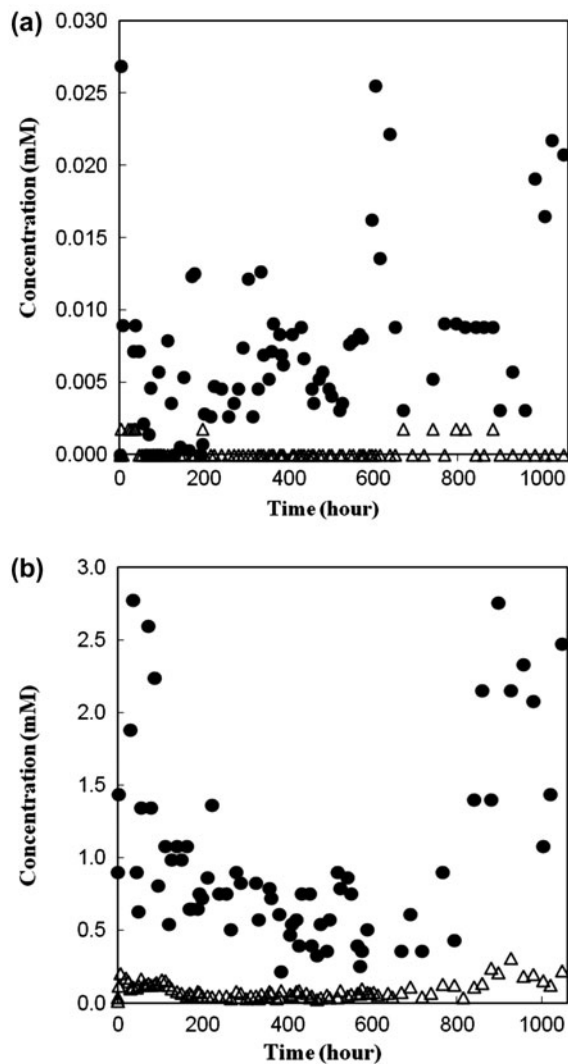


Fig. 7. Concentrations of total dissolved iron (•) and ferrous iron (Δ) in effluent from (a) column 2 and (b) column 3.

dissolution of metal. In other words, anions are adsorbed on the surface of metal-forming stable complexes of the $\text{Fe}-\text{Cl}_{\text{ads}}^-$ type, and iron dissolution is impeded, when the concentration of complexes $\text{Fe}-\text{H}_2\text{O}$ is low [29,30]. This complex formation may be the reason for variation of the chloride concentrations in samples from column 3. Initially, a low concentration of chloride in the water favors the dissolution of iron and TCE dechlorination. This promotes an increase in chloride ions as well as its interaction with the metal and leads to depletion of the reactive surface of iron metal.

3.4. The pH values

The pH values of three columns are presented in Fig. 9. The pH of column 1 and column 2 were similar

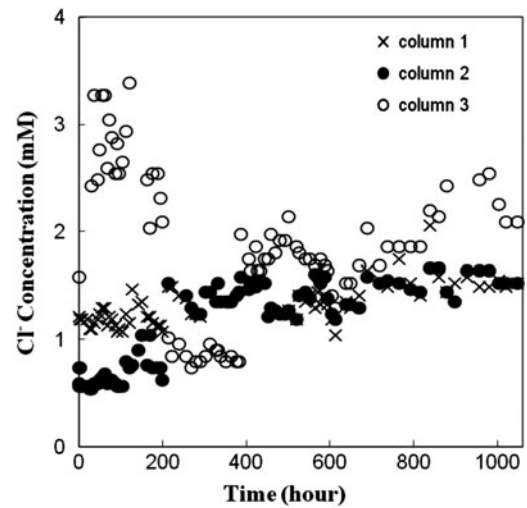


Fig. 8. Chloride content in effluent of the columns (column 1 (\times), column 2 (\bullet), column 3 (\circ)) with time.

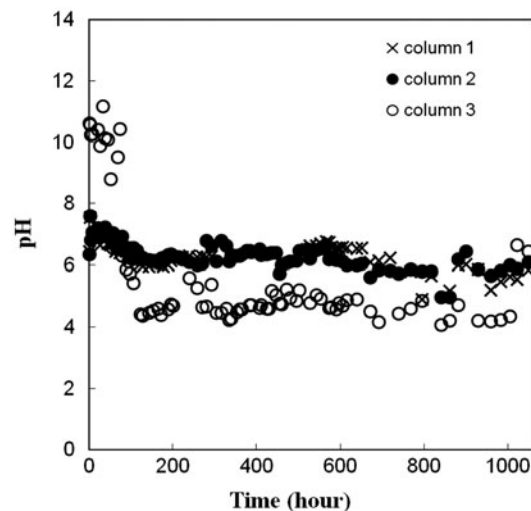


Fig. 9. The pH values vs. time passed through column 1 (\times), column 2 (\bullet), column 3 (\circ).

between five and seven. The values for column 3 were high at the initial stage of the experiment, but decreased rapidly and then remained at a lower range. H^+ ions are released by oxidation of water (Eq. (6)) near, and at the anode and derive a low pH, when external electric current is supplied. In the vicinity of the cathode, water reduction occurred, and the generation of hydroxide ions (Eq. (1)) increased the pH. Since all samples were collected from outlets near the cathode, high pH analogous to other research [25] was expected for column 3. However, low values in the range of 4–5 were observed, except for the pH before 70 h of reaction time. This difference may be explained

as the effect of a sharp acid–base front developing due to water electrolysis. The acid front will move toward the cathode by migration, diffusion, and advection. The base front will migrate in the opposite direction toward the anode. The H^+ ions will dominate the system chemistry; hence, the 1.75 times higher ionic mobility of H^+ ions than that of OH^- ions [31]. Moreover, water flows from anode to cathode, so the acid front was transported with the hydraulic flow of the water.

3.5. Electrical conductivity

The electrical conductivity of the control column and column 2 were retained at approximately $230 \mu S cm^{-1}$. However, the electrical conductivity of column 3 was higher than the others, in the range of 250 – $280 \mu S cm^{-1}$, because many dissolved ions were produced by rapid oxidation of ZVI due to the external electric current supply. Furthermore, H^+ ions and OH^- ions were generated by water electrolysis (Eq. (1) and (6)). These two ions have a higher equivalent conductance (350.1 and $199.2 S\text{-}cm\text{eq}^{-1}$, respectively) than that of other ions [32].

4. Conclusions

We evaluated an electrochemical PRB for dechlorination of TCE in groundwater. The performance of a typical PRB structure comprised of ZVI, and sand was compared with that of bipolar packed-bed electrodes derived from the typical PRB by imposing an external current.

Approximately, 10 times greater concentrations of TCE (average: 0.1 mM) were reduced through the column with external current, whereas the column without current showed a removal concentration of 0.01 mM . The dominant dechlorinated hydrocarbons, the by-products of TCE degradation, from the columns without and with current were ethylene and ethane, respectively. This indicated that the supplied current accelerated the production of electrons from iron oxidation and water electrolysis. ZVI was coated with (hydro)oxides with increased time, therefore, TCE removal rate decreased. However, in the latter stages of the experiment, the iron oxides may allow electron transfer to occur and may support increased TCE reduction rates. The total dissolved iron and chloride in the effluent increased with increasing removal concentrations of TCE, and vice versa.

This finding implies that inducing current to ZVI improves the removal of TCE, even when ZVI has inactive surfaces, and the electrical conductivity is in the range of 250 – $280 \mu S cm^{-1}$. Although more studies are

needed to investigate characteristics and configurations for system optimization, these findings have important implications for developing a bipolar electrode packed-bed as an alternative to a typical PRB.

Acknowledgment

The authors would like to thank the Seoul Business Agency for financial support under Grant No. PA100095 (Commercialization of Patented Technologies Program).

References

- [1] T. Umezumi, J. Yonemoto, Y. Soma, T. Miura, Behavioral effects of trichloroethylene and tetrachloroethylene in mice, *Pharmacol. Biochem. Behav.* 58(3) (1997) 665–671.
- [2] R.E. Watson, C.F. Jacobson, A.L. Williams, W.B. Howard, J.M. DeSesso, Trichloroethylene-contaminated drinking water and congenital heart defects: A critical analysis of the literature, *Reprod. Toxicol.* 21(2) (2006) 117–147.
- [3] H.H. Russell, J.E. Matthews, G.W. Sewell, Ground Water Issue: TCE Removal from Contaminated Soil and Ground Water, US Environmental Protection Agency, EPA/540/S-92/002, 1992.
- [4] W.A. Chiu, J.C. Caldwell, N. Keshava, C.S. Scott, Key scientific issues in the health risk assessment of trichloroethylene, *Environ. Health Perspect.* 144(9) (2006) 1445–1449.
- [5] H. Shen, J.T. Wilson, Trichloroethylene removal from groundwater in flow-through columns simulating a permeable reactive barrier constructed with plant mulch, *Environ. Sci. Technol.* 41(11) (2007) 4077–4083.
- [6] K. Ritter, M.S. Odziemkowski, R.W. Gillham, An *in situ* study of the role of surface films on granular iron in the permeable iron wall technology, *J. Contam. Hydrol.* 55(1–2) (2002) 87–111.
- [7] R. Baciocchi, M.R. Boni, L. D'Aprile, Characterization and performance of granular iron as reactive media for TCE degradation by permeable reactive barriers, *Water Air Soil Pollut.* 149(1) (2003) 211–226.
- [8] G.P. Grant, B.H. Kueper, The influence of high initial concentration aqueous-phase TCE on the performance of iron wall systems, *J. Contam. Hydrol.* 74(1–4) (2004) 299–312.
- [9] A.D. Henderson, A.H. Demond, Long-term performance of zero-valent iron permeable reactive barriers: A critical review, *Environ. Eng. Sci.* 24(4) (2007) 401–423.
- [10] R.M. Powell, D.W. Blowes, R.W. Gillham, D. Schultz, T. Sivavee, R.W. Puls, J.L. Vogan, P.D. Powell, R. Landis, Permeable Reactive Barrier Technologies for Contaminant Remediation. US Environmental Protection Agency, EPA/600/R-98/125, 1998.
- [11] S.R. Al-Abed, Y. Fang, Influences of pH and current on electrolytic dechlorination of trichloroethylene at a granular-graphite packed electrode, *Chemosphere* 64(3) (2006) 462–469.
- [12] S. Jin, P.H. Fallgren, Electrically induced reduction of trichloroethene in clay, *J. Hazard. Mater.* 173(1–3) (2010) 200–204.
- [13] Y. Roh, S.Y. Lee, M.P. Elless, H.S. Moon, Electro-enhanced remediation of trichloroethene-contaminated groundwater using zero-valent iron, *J. Environ. Sci. Health., Part A* 35(7) (2000) 1061–1076.
- [14] J.W. Moon, H.S. Moon, H. Kim, Y. Roh, Remediation of TCE-contaminated groundwater using zero valent iron and direct current: Experimental results and electron competition model, *Environ. Geol.* 48(6) (2005) 805–817.
- [15] C.C. Liu, S.F. Liao, D.H. Tseng, Effects of the electrode arrangements on reductive dechlorination of trichloroethylene in an electro-enhanced iron wall, *Environ. Technol.* 27(6) (2006) 683–693.

- [16] G. Chen, Electrochemical technologies in wastewater treatment, *Sep. Purif. Technol.* 38(1) (2004) 11–41.
- [17] M.Y.A. Mollah, P. Morkovsky, J.A.G. Gomes, M. Kesmez, J. Parga, D.L. Cocke, Fundamentals, present and future perspectives of electrocoagulation, *J. Hazard. Mater.* 114(1–3) (2004) 199–210.
- [18] D. Rahner, G. Ludwig, J. Röhrs, Electrochemically induced reactions in soils—A new approach to the in-situ remediation of contaminated soils? Part 1: The microconductor principle *Electrochim. Acta* 47(9) (2002) 1395–1403.
- [19] L.S. Clesceri, A.E. Greenberg, A.D. Eaton, *Standard Methods, Examination of Water and Wastewater*, 20th ed., American Public Health Association (APHA), Amsterdam, 1998.
- [20] N.D. Berge, C.A. Ramsburg, Iron-mediated trichloroethene reduction within nonaqueous phase liquid, *J. Contam. Hydrol.* 118 (2010) 105–116.
- [21] C.J. Lin, S.L. Lo, Effects of iron surface pretreatment on sorption and reduction kinetics of trichloroethylene in a closed batch system, *Water Res.* 39(6) (2005) 1037–1046.
- [22] C.C. Liu, D.H. Tseng, C.Y. Wang, Effects of ferrous ions on the reductive dechlorination of trichloroethylene by zero-valent iron, *J. Hazard. Mater.* 136(3) (2006) 706–713.
- [23] V.A. Juvekar, R.S. Patil, A.V.P. Gurumoorthy, A.Q. Contractor, Analysis of multiple reactions on a bipolar electrode, *Ind. Eng. Chem. Res.* 48(21) (2009) 9441–9456.
- [24] L.J. Matheson, P.G. Tratnyek, Reductive dehalogenation of chlorinated methanes by iron metal, *Environ. Sci. Technol.* 28 (12) (1994) 2045–2053.
- [25] J. Röhrs, G. Ludwig, D. Rahner, Electrochemically induced reactions in soils—A new approach to the in-situ remediation of contaminated soils? Part 2: Remediation experiments with a natural soil containing highly chlorinated hydrocarbons *Electrochim. Acta* 47(9) (2002) 1405–1414.
- [26] W.A. Arnold, A.L. Roberts, Pathways and kinetics of chlorinated ethylene and chlorinated acetylene reaction with Fe(0) particles, *Environ. Sci. Technol.* 34(9) (2000) 1794–1805.
- [27] A.L. Roberts, L.A. Totten, W.A. Arnold, D.R. Burris, T.J. Campbell, Reductive elimination of chlorinated ethylenes by zero-valent metals, *Environ. Sci. Technol.* 30(8) (1996) 2654–2659.
- [28] A.R. Gavaskar, Design and construction techniques for permeable reactive barriers, *J. Hazard. Mater.* 68(1–2) (1999) 41–71.
- [29] A.Y. Aleksanyan, I.I. Reformatskaya, A.N. Podobaev, The effect of chloride and sulfate anions on the iron dissolution rate in neutral and nearly neutral media, *Prot. Met.* 43(2) (2007) 125–128.
- [30] A.N. Podobaev, Effect of chloride ions on the rate of iron dissolution in weakly acid sulfate solution, *Prot. Met.* 41(6) (2005) 548–552.
- [31] B. Narasimhan, R.S. Ranjan, Electrokinetic barrier to prevent subsurface contaminant migration: Theoretical model development and validation, *J. Contam. Hydrol.* 42(1) (2000) 1–17.
- [32] C.N. Sawyer, P.L. McCarty, G.F. Parkin, *Chemistry for Environmental Engineering and Science*, 5th ed., McGraw-Hill, New York, NY, 2003.